*Int. J. Heat Mass Transfer.* Vol. 29, No. 1, pp. 47–58, 1986
Printed in Great Britain

0017–9310/86 $3.00 + 0.00


# A general method for the solution of inverse heat conduction problems with partially unknown system geometries

C. K. HSIEH and ALAIN J. KASSAB
Department of Mechanical Engineering, University of Florida, Gainesville, FL 32611, U.S.A.

(*Received* 13 *July* 1984 *and in final form* 15 *July* 1985)

**Abstract**—An auxiliary problem is introduced in the solution of inverse heat conduction problems with geometries not fully specified. Resolving the position of the unknown boundary subject to a Dirichlet condition leads to the solution of a nonlinear algebraic equation. Imposing Neumann or Robin conditions at the unknown boundary requires the solution of a first-order nonlinear, ordinary differential equation. The method yields accurate results for exact data, while measurement errors render the Neumann problem insoluble. The Dirichlet and Robin problems are still solvable, and for these problems, the errors in the investigated boundaries increase with their depth, a nature of the problem being investigated.

## INTRODUCTION

TRADITIONAL heat conduction problems are concerned with the determination of the temperature distribution in a body when the system geometry, governing equation, and initial and boundary conditions are all known. Problems of this type are called direct or regular problems. Another class of problems arises when one of those conditions just mentioned is either unknown or not fully specified, and the unknown is solved with the help of an extra condition [1–22]. For example, when the governing equation is given and the boundary conditions are overspecified at one of the boundaries, but the system geometry is not fully known, and the missing portion of the geometry is being investigated in the solution, then the problem becomes an inverse problem. This problem finds practical applications in nondestructive testing of flaws and cavities, in which the surface temperature of a body is measured by infra-red scanning. The scanned surface also dissipates heat by convection. Two conditions are thus available at the same surface. The additional information provided by the measured temperature is used along with the others to determine fully the geometry of the investigated body. The present inverse problem forms the theoretical basis for developing infra-red computerized axial tomography in competition with the X-ray computerized axial tomography (X-ray CAT) that is now prevalent in the medical technology.

Several methods have been developed for the solution of this inverse problem. A pattern recognition technique has been proposed [10, 11, 15]. A numerical searching scheme has been developed to solve this problem when a prescribed temperature is imposed at the unknown boundary [17, 20]. For a prescribed heat flux at the unknown boundary, a different method of intrinsic matching was found useful [18].

A close examination of the developed methods reveals that they are only useful if the unknown boundary is made up of line segments that are parallel to the orthogonal axes of the investigated system. For instance, these methods can only detect rectangular cavities in Cartesian coordinates. Furthermore, the solution methods developed vary with the type of condition appearing at the unknown boundary. There is a lack of a general approach to the solution of this problem.

It is the purpose of this paper to present a general solution method. As will be shown, the method to be developed is independent of the type of condition imposed at the unknown boundary. Furthermore, the method is valid for any configuration of this boundary as long as it has a smooth curvature and is located close to the surface.

## DESCRIPTION OF THE INVERSE PROBLEM

Consider the two-dimensional systems shown in Fig. 1. The position of the irregular boundary is unknown in each case. One of three situations may physically arise at this irregular boundary to represent (i) a Dirichlet condition (prescribed temperature), (ii) a Neumann condition (prescribed heat flux), or (iii) a Robin condition (convective heat exchange with a source at a prescribed temperature). The opposite surface at $y = 0$ or $r = R_0$ dissipates heat to the surrounding at zero temperature (a homogeneous Robin condition). The temperature profile along this surface is also measured by infra-red scanning and is thus known (a nonhomogeneous Dirichlet condition). The conditions at $x = 0$ and $L$ of the plane slab or those conditions in the $\phi$ direction in the cylinder and the sphere are all homogeneous. Specifically, the plane slab can be divided along the $x$ direction at sections where the temperature gradients are negligibly small; see Fig. 1(a). These sections are considered adiabatic planes (their validity will be examined later). As for the cylinder and

## NOMENCLATURE

$A_0, A_n, C_n, D_0, E_n, F_n, G_n$ coefficients in the orthogonal series expansions of the temperature
$Bi$ Biot number, $hL/k$ or $hR_o/k$
$[C]$ column vector defined by equation (27)
$d$ thickness of the slab in the auxiliary problem
$g$ constant heat flux at $S_4$
$h$ convective heat transfer coefficient
$[J]$ Jacobian matrix with elements defined by equations (24)–(26) and (29)–(31)
$k$ thermal conductivity
$L$ length of slab
$l, m$ direction cosines
$M$ number of points discretized along $\xi$ axis
$N$ number of terms used in the orthogonal series expansions of the temperature
$\hat{n}$ normal vector
$P$ Legendre polynomial or amplification factor
$R$ residual
$R_0$ outer radius of the cylinder or sphere
$r$ radius coordinate or position vector
$S$ surface
$T$ temperature
$U, V$ functions of $u, v$, respectively
$u, v, x, y$ coordinates
$[Z]$ correction vector expressed in equation (23).

Greek symbols
$\delta$ thickness of the slab in the auxiliary problem
$\varepsilon$ truncation error
$\eta$ dimensionless thickness, $y/L$
$\theta$ dimensionless temperature defined by equations (10), (11) and (12)
$\xi$ dimensionless length, $x/L$
$\rho$ dimensionless radius, $r/R_0$
$\phi$ polar angle.

Subscripts
AC refers to AC component in the electrical analogy
DC refers to DC component in the electrical analogy
$i$ refers to the location of point along $\xi$ axis
0 refers to the temperature imposed at the unknown boundary
s refers to the source temperature with which the unknown boundary exchanges heat
$\infty$ refers to ambient.

Superscripts
$l$ refers to $l$th correction in the Newton–Raphson method
$'$ refers to derivative.

the sphere, the temperature must be finite and single valued in the $\phi$ direction.

It is assumed that the systems are stationary, in steady state, and have no sources or sinks. Their thermal conductivities are constant. Under these conditions, the governing equation describing the heat flow is a Laplace equation.

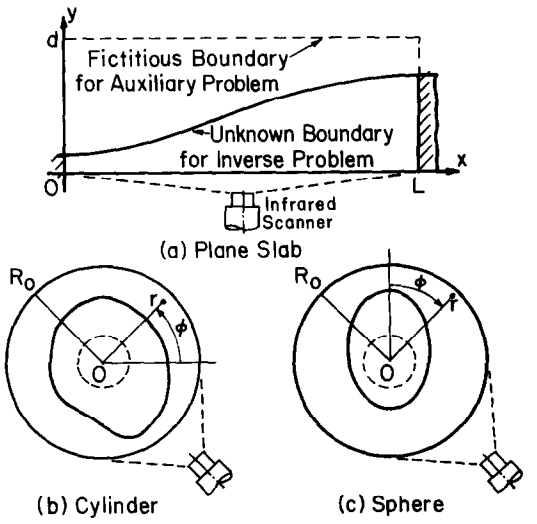


FIG. 1. Systems investigated in the solution of the inverse problem.

The inverse problem mentioned above can be considered a Cauchy problem because out of three possible conditions (Dirichlet, Neumann, or Robin) imposed at any boundary, only two conditions are independent. Then, a prescription of the Dirichlet and Robin conditions at the outer (scanned) surface in the present inverse problem is equivalent to the specification of Cauchy conditions at this surface [23]. For the present study, these Cauchy conditions are used to locate the unknown boundary in the inverse problem, and these Cauchy conditions are also the result of the condition that appears at the unknown boundary as well as the geometry of this boundary.

## SOLUTION METHODOLOGY

The inverse problems illustrated in Fig. 1 can be solved by considering an auxiliary problem. Take the plane slab for example. The auxiliary problem has boundaries at $y = 0$ and $x = 0$ and $L$ coincident with those of the inverse problem; however, the remaining boundary of this auxiliary problem extends beyond the

irregular boundary of the inverse problem and terminates at the dashed line; see Fig. 1(a). Hence, the auxiliary problem is bounded by a set of regular boundaries. For this auxiliary problem, it is not necessary to specify the position of the fictitious (dashed line) boundary, nor is it necessary to prescribe its condition. However, the assumptions made earlier for the inverse problem are still applicable to the solution of this auxiliary problem.

The auxiliary problem can be solved with the use of the separation of variables technique. The homogeneous conditions mentioned earlier can be used to derive the temperature as a series of the form

$$T(\bar{r}) = \sum_{n=0}^{\infty} C_n U(u) V(v) \tag{1}$$

where $\bar{r}$ denotes a position vector with components $u$ and $v$. $U$ and $V$ are functions of $u$ and $v$, respectively.

The next step in the solution is to use a nonhomogeneous boundary condition to determine the coefficients $C_n$, in equation (1); it is at this point that the solution of the auxiliary problem departs from the traditional method of solution. The reason is that a regular problem will arise if the nonhomogeneous condition is taken from the fictitious boundary; see Fig. 2. However, since the condition on this boundary is unknown at this moment, one is forced to use the nonhomogeneous condition (scanned temperature) at $y = 0$ to solve for these coefficients. Because of the elliptic nature of the governing equation, it will be shown later that the Fourier coefficients can be determined independently of the location of the nonhomogeneous condition used to resolve them.

It is noted that the irregular boundary of the original inverse problem is now located inside the system domain of the auxiliary problem; see Fig. 1(a). Since the auxiliary problem has just been solved, finding the position of the irregular boundary is reduced to the task of locating the position of the contour line in the auxiliary domain where the condition imposed at the irregular boundary is satisfied. For example, if a Dirichlet condition is imposed at the irregular boundary of the plane slab, then the position of this irregular boundary is located by searching for the equivalent isotherm inside the domain of the auxiliary problem.

The location of the irregular contour line in the auxiliary problem is accomplished through an inverse collocation scheme. The derived temperature expression for the auxiliary problem is forced to satisfy the condition prescribed at the irregular contour. The solution now depends on the condition that is imposed at the contour. A nonlinear algebraic equation results if a Dirichlet condition appears at the contour. A Neumann or a Robin condition at the contour will lead to nonlinear ordinary differential equations. In either case, the Newton–Raphson method can be used to numerically locate the unknown boundary in the inverse problem.

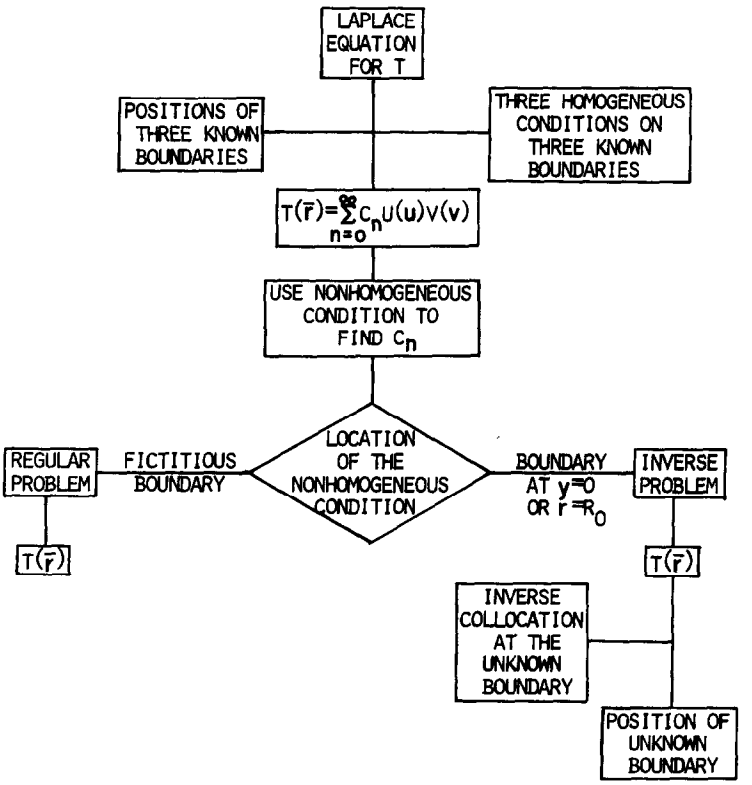


FIG. 2. Logic for solution of the inverse problem.

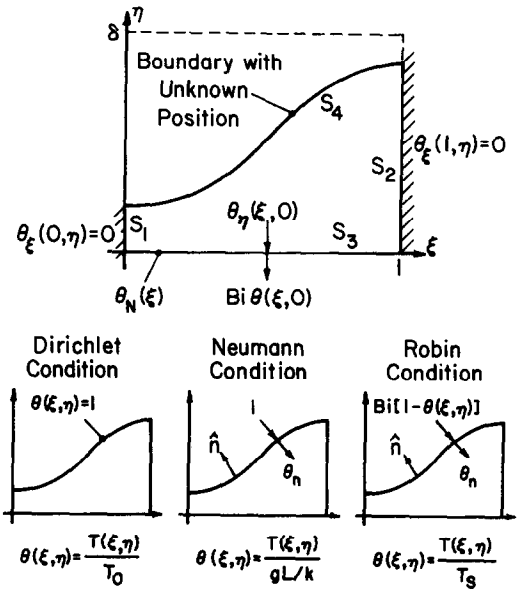


FIG. 3. A diagram showing the three problems solved for the plane slab example.

## EXAMPLE

An example is provided in this section to illustrate a practical application of the developed methodology. Consider the plane slab shown in Fig. 1, which is redrawn in Fig. 3. The governing equation and boundary conditions for this problem are formulated dimensionlessly as follows:

Governing equation

$$\nabla^2\theta(\xi,\eta)=0. \tag{2}$$

Boundary conditions

$S_1$:

$$\theta_\xi(0,\eta)=0 \quad \text{(adiabatic condition)} \tag{3}$$

$S_2$:

$$\theta_\xi(1,\eta)=0 \quad \text{(adiabatic condition)} \tag{4}$$

$S_3$ (two conditions are given):

$$\theta_\eta(\xi,0)=Bi\theta(\xi,0) \quad \text{(convective condition)} \tag{5}$$

$$\theta(\xi,0)=\theta_N(\xi) \quad \text{(scanned temperature)} \tag{6}$$

where equation (6) is an extra condition. The objective of this problem is to locate the unknown boundary $S_4$; along this boundary there may be:

a Dirichlet condition

$$\theta[\xi,f(\xi)]=1, \tag{7}$$

a Neumann condition

$$\theta_n[\xi,f(\xi)]=1, \tag{8}$$

or a Robin condition

$$\theta_n[\xi,f(\xi)]=Bi\{1-\theta[\xi,f(\xi)]\}. \tag{9}$$

In those equations given above

$\xi=x/L$, $\eta=y/L$, $Bi=hL/k$ = Biot number

$h$ is the convective coefficient, and $k$ is the thermal conductivity.

The example given here will be divided into three subproblems in which each has a different condition imposed at $S_4$. The dimensionless temperature, $\theta$, is defined differently for these subproblems. For example, a Dirichlet condition at $S_4$ requires that $\theta$ be defined as

$$\theta(\xi,\eta)=\frac{T(\xi,\eta)-T_\infty}{T_0-T_\infty}=\frac{T(\xi,\eta)}{T_0}. \tag{10}$$

For a Neumann condition at $S_4$,

$$\theta(\xi,\eta)=\frac{T(\xi,\eta)-T_\infty}{(gL/k)}=\frac{T(\xi,\eta)}{(gL/k)}. \tag{11}$$

For a Robin condition at $S_4$.

$$\theta(\xi,\eta)=\frac{T(\xi,\eta)-T_\infty}{T_s-T_\infty}=\frac{T(\xi,\eta)}{T_s}. \tag{12}$$

These expressions relate $\theta$ with the actual temperature $T$, and in these expressions the ambient temperature, $T_\infty$, has been taken to be zero; $g$ is the heat flux.

For all three subproblems, equation (2) can be solved with the use of conditions (3)–(5) to give

$$\theta(\xi,\eta)=A_0(Bi\eta+1)+\sum_{n=1}^{\infty}A_n \times\left(\frac{n\pi}{Bi}\cosh n\pi\eta+\sinh n\pi\eta\right)\cos n\pi\xi. \tag{13}$$

At $\eta=0$, equation (13) reduces to

$$\theta(\xi,0)=A_0+\sum_{n=1}^{\infty}A_n\frac{n\pi}{Bi}\cos n\pi\xi. \tag{14}$$

This equation will be used to least-squares fit the scanned surface temperature data, $\theta_N(\xi)$, equation (6), in order to find the coefficients $A_0$ and $A_n$ in the Fourier series expansion of the temperature. The solution developed so far is common to all three subproblems; what follows now depends on the type of condition imposed at $S_4$.

*Dirichlet condition*

Imposing a Dirichlet condition at the unknown boundary $S_4$ requires that the nonlinear equation

$$1-A_0(Bi\eta+1)-\sum_{n=1}^{N-1}A_n \times\left(\frac{n\pi}{Bi}\cosh n\pi\eta+\sinh n\pi\eta\right)\cos n\pi\xi=0 \tag{15}$$

be satisfied at each point $(\xi,\eta)$ along the unknown boundary. Hence, the position of the unknown boundary of the Dirichlet-condition problem can be found by solving (15) for $\eta$ as a function of $\xi$. Because analytical solution of (15) is not possible, one must resort to numerical methods; the position of the boundary is determined at discrete points $\xi_i$ by solving (15) for the associated roots $\eta_i$. The Newton–Raphson method is used to numerically determine these roots. In

this method, the $(l+1)$th corrected root is expressed as

$$\eta_i^{(l+1)} = \eta_i^{(l)} + Z_i^{(l)} \tag{16}$$

where

$$Z_i^{(l)} = \frac{1 - A_0(Bi\eta_i^{(l)} + 1) - \sum_{n=1}^{N-1} A_n \left( \frac{n\pi}{Bi} \cosh n\pi\eta_i^{(l)} + \sinh n\pi\eta_i^{(l)} \right) \cos n\pi\xi_i}{A_0 Bi + \sum_{n=1}^{N-1} A_n n\pi \left( \frac{n\pi}{Bi} \sinh n\pi\eta_i^{(l)} + \cosh n\pi\eta_i^{(l)} \right) \cos n\pi\xi_i}. \tag{17}$$

In practice, a sufficiently accurate starting value $\eta_i^{(0)}$ is provided by a simple brute-force algorithm in which the neighborhood of the root is determined by a bisection method.

*Neumann condition*

For a Neumann condition at the unknown boundary, the expression to be satisfied is

$$1 - A_0 Bim - \sum_{n=1}^{N-1} A_n n\pi \left[ m \left( \frac{n\pi}{Bi} \sinh n\pi\eta + \cosh n\pi\eta \right) \cos n\pi\xi - l \left( \frac{n\pi}{Bi} \cosh n\pi\eta + \sinh n\pi\eta \right) \sin n\pi\xi \right] = 0 \tag{18}$$

where $l$ and $m$ are the direction cosines of the outward-drawn normal at the unknown boundary. These direction cosines are functions of the position $\xi$.

It is necessary to express these direction cosines in terms of the local slope $(\eta')$ of the unknown boundary,

$$l(\xi) = -\frac{\eta'}{(1+\eta'^2)^{1/2}}, \quad m(\xi) = \frac{1}{(1+\eta'^2)^{1/2}}. \tag{19}$$

Substitution of (19) into the boundary equation (18) yields a nonlinear differential equation

$$(1+\eta'^2)^{1/2} - A_0 Bi - \sum_{n=1}^{N-1} A_n n\pi \left[ \left( \frac{n\pi}{Bi} \sinh n\pi\eta + \cosh n\pi\eta \right) \cos n\pi\xi + \eta' \left( \frac{n\pi}{Bi} \cosh n\pi\eta + \sinh n\pi\eta \right) \sin n\pi\xi \right] = 0 \tag{20}$$

which cannot be solved without use of numerical methods.

In the numerical solution of (20), the $\xi$-axis is discretized into $M$ equally spaced points. Central differencing is used to approximate $\eta'$, and equation (20) is recast as

$$\left[ 1 + \left( \frac{\eta_{i+1} - \eta_{i-1}}{2\Delta\xi} \right)^2 \right]^{1/2} - A_0 Bi - \sum_{n=1}^{N-1} A_n n\pi \times \left[ \left( \frac{n\pi}{Bi} \sinh n\pi\eta_i + \cosh n\pi\eta_i \right) \cos n\pi\xi_i + \left( \frac{\eta_{i+1} - \eta_{i-1}}{2\Delta\xi} \right) \times \left( \frac{n\pi}{Bi} \cosh n\pi\eta_i + \sinh n\pi\eta_i \right) \sin n\pi\xi_i \right] = 0 \tag{21}$$

for $i = 1$ to $M$. The next step in the solution is to resolve the problem posed by the coupling of $\eta_i$ with its neighboring points $\eta_{i-1}$ and $\eta_{i+1}$; both of which being unknown at the moment. Also notice that equation (21) is nonlinear.

The Newton–Raphson method is again useful to solve this problem. In this method, the corrected solution for $\eta_i$ is again expressed as equation (16). However, this equation now becomes a matrix equation of order $M$, for which the iterative procedure requires an initial trial vector $\eta_i^{(l)}$ that is accurate enough to assure a convergent iteration. A procedure is described below to evaluate this vector.

(1) The positions $\eta_1$ and $\eta_M$ at $\xi = 0$ and 1 can be found by making use of the adiabatic conditions imposed there; see Fig. 3. Such conditions are physically possible when the slope of the boundary $S_4$ vanishes at these points. Consequently, the central differencing terms in equation (21) vanish at these points, and $\eta_1$ and $\eta_M$ are uncoupled from their neighboring points. This allows the positions $\eta_1$ and $\eta_M$ to be found directly from equation (21).

(2) With the position of $\eta_l$ determined from step (1) above, the position of $\eta_2$ can be estimated by changing the central difference terms in equation (21) to backward difference, that is,

$$\left[ 1 + \left( \frac{\eta_i - \eta_{i-1}}{\Delta\xi} \right)^2 \right]^{1/2} - A_0 Bi - \sum_{n=1}^{N-1} A_n n\pi \times \left[ \left( \frac{n\pi}{Bi} \sinh n\pi\eta_i + \cosh n\pi\eta_i \right) \cos n\pi\xi_i + \left( \frac{\eta_i - \eta_{i-1}}{\Delta\xi} \right) \times \left( \frac{n\pi}{Bi} \cosh n\pi\eta_i + \sinh n\pi\eta_i \right) \sin n\pi\xi_i \right] = 0. \tag{22}$$

Notice that the position of $\eta_i$ is now only related to $\eta_{i-1}$; thus, using the previously found $\eta_1$ as an estimate for $\eta_2$ enables the position of $\eta_2$ to be obtained via the Newton–Raphson method. This procedure is marched down the contour $S_4$ from $\eta_2$ to $\eta_{M-1}$. The estimation required to start the iteration at each point $\eta_i$(for $i \geqslant 3$) is provided by extrapolating the calculated values for the previous points $\eta_{i-1}$ and $\eta_{i-2}$, i.e. $\eta_i = 2\eta_{i-1} - \eta_{i-2}$.

(3) The position of the boundary $S_4$ found in step (2) above is inaccurate because it is based on the use of backward difference for $\eta'$ in (22). However, this position is adequate for use as the trial vector in the iterative procedure using the central difference for $\eta'$.

The correction vector $[Z]$ for the Neumann-condition problem is evaluated by solving the following related equation

$$[J][Z] = -[C] \tag{23}$$

where $[J]$ is the Jacobian matrix with elements

$$J_{i,i-1}=\frac{\eta_{i+1}-\eta_{i-1}}{4(\Delta\xi)^2}\left[1+\left(\frac{\eta_{i+1}-\eta_{i-1}}{2\Delta\xi}\right)^2\right]^{-1/2}+\sum_{n=1}^{N-1}A_n\frac{n\pi}{2\Delta\xi}\left[\left(\frac{n\pi}{Bi}\cosh n\pi\eta_i+\sinh n\pi\eta_i\right)\sin n\pi\xi_i\right] \tag{24}$$

$$J_{i,i}=-\sum_{n=1}^{N-1}A_n(n\pi)^2\times\left[\left(\frac{n\pi}{Bi}\cosh n\pi\eta_i+\sinh n\pi\eta_i\right)\cos n\pi\xi_i+\left(\frac{\eta_{i+1}-\eta_{i-1}}{2\Delta\xi}\right)\times\left(\frac{n\pi}{Bi}\sinh n\pi\eta_i+\cosh n\pi\eta_i\right)\sin n\pi\xi_i\right] \tag{25}$$

$$J_{i,i+1}=-J_{i,i-1} \tag{26}$$

for $i=1$ to $M$. The elements of the column vector $[C]$ are

$C_i=$ the LHS of equation (21) evaluated at position $i$. (27)

Also notice that $\eta_i$ is only related to $\eta_{i-1}$ and $\eta_{i+1}$ in equation (21); the Jacobian matrix is therefore tridiagonal.

There are two ways by which the correction vector $[Z]$ can be computed. One could treat the point $\eta_1$ and $\eta_M$ calculated in step (1) as exact. Then $z$ will be zero for points 1 and $M$; consequently, the index $i$ in equations (24)–(26) runs from 2 to $M-1$, and the Jacobian matrix is reduced to a $(M-2)\times(M-2)$ matrix. For the convenience of later discussion, this method of treating the ends as fixed, anchored points is called the ends-anchored method (EAM). Alternatively, the ends may be treated as floating points. Then $z_1$ and $z_M$ are retained in equation (23), and the Jacobian matrix is still taken to be a $M\times M$ matrix. This method of treating the endpoints as floating points is referred to as the ends-floating method (EFM). The accuracy of both methods will be examined later.

*Robin condition*

Imposing the Robin condition at the unknown boundary requires that the following expression be satisfied at the boundary

$$Bi(1+\eta'^2)^{1/2}-A_0Bi[1+(Bi\eta+1)(1+\eta'^2)^{1/2}]-\sum_{n=1}^{N-1}A_n n\pi\left\{\left(\frac{n\pi}{Bi}\sinh n\pi\eta+\cosh n\pi\eta\right)\cos n\pi\xi+\left(\frac{n\pi}{Bi}\cosh n\pi\eta+\sinh n\pi\eta\right)\left[\eta'\sin n\pi\xi+(1+\eta'^2)^{1/2}\times\frac{Bi}{n\pi}\cos n\pi\xi\right]\right\}=0. \tag{28}$$

The procedure required to locate this boundary for the Robin-condition problem is identical to that for the Neumann-condition problem. In fact, equation (28) is the counterpart of equation (20) in the Neumann problem. The counterparts of equations (24), (25) and (26) are, respectively,

$$J_{i,i-1}=Bi[A_0(Bi\eta_i+1)-T_s]\times\frac{\eta_{i+1}-\eta_{i-1}}{4(\Delta\xi)^2}\left[1+\left(\frac{\eta_{i+1}-\eta_{i-1}}{2\Delta\xi}\right)^2\right]^{-1/2}+\sum_{n=1}^{N-1}A_n\frac{n\pi}{2\Delta\xi}\left(\frac{n\pi}{Bi}\cosh n\pi\eta_i+\sinh n\pi\eta_i\right)\left\{\sin n\pi\xi_i+\frac{\eta_{i+1}-\eta_{i-1}}{2\Delta\xi}\left[1+\left(\frac{\eta_{i+1}-\eta_{i-1}}{2\Delta\xi}\right)^2\right]^{-1/2}\frac{Bi}{n\pi}\cos n\pi\xi_i\right\} \tag{29}$$

$$J_{i,i}=-A_0Bi^2\left[1+\left(\frac{\eta_{i+1}-\eta_{i-1}}{2\Delta\xi}\right)^2\right]^{1/2}-\sum_{n=1}^{N-1}A_n(n\pi)^2\left[\left(\frac{n\pi}{Bi}\cosh n\pi\eta_i+\sinh n\pi\eta_i\right)\cos n\pi\xi_i+\left(\frac{n\pi}{Bi}\sinh n\pi\eta_i+\cosh n\pi\eta_i\right)\left\{\left(\frac{\eta_{i+1}-\eta_{i-1}}{2\Delta\xi}\right)\sin n\pi\xi_i+\left[1+\left(\frac{\eta_{i+1}-\eta_{i-1}}{2\Delta\xi}\right)^2\right]^{1/2}\frac{Bi}{n\pi}\cos n\pi\xi_i\right\}\right] \tag{30}$$

$$J_{i,i+1}=-J_{i,i-1}. \tag{31}$$

## CONVERGENCE, UNIQUENESS, STABILITY AND CONSISTENCY

*Convergence*

It is shown that the Fourier series given by equation (14) converges. Integrating equation (14) twice by parts and taking $M$ to be $|\theta''(\xi,0)|<M$ where $\theta''(\xi,0)$ is continuous in the interval $0\leqslant\xi\leqslant1$ gives the result that the Fourier series corresponding to equation (14) is at most equal to the corresponding term of the series

$$|A_0|+\frac{2M}{\pi^2}\left(1+\frac{1}{2^2}+\frac{1}{3^2}+\cdots\right)$$

which is convergent. By using the Weierstrass test, the series can also be shown to converge uniformly.

*Uniqueness*

It has been established that solution to a Laplace equation is unique [24]. It remains to be shown that the coefficients, evaluated based on the use of the scanned temperature given at $\eta=0$, are as good as those evaluated by using the temperature at the fictitious boundary, $\eta=\delta$, as has been done in common practice. Attention is directed to equation (13) which may be recast as

$$\theta(\xi,\eta)=\theta_{DC}(\eta)+\sum_{n=1}^{\infty}\theta_{AC,n}(\xi,\eta) \tag{32}$$

where

$$\theta_{DC}(\eta)=A_0(Bi\eta+1) \tag{33}$$

and

$$\theta_{AC,n}(\xi, \eta) = A_n \frac{n\pi}{Bi}\left(\cosh n\pi\eta + \frac{Bi}{n\pi}\sinh n\pi\eta\right)\cos n\pi\xi. \tag{34}$$

These $\theta_{DC}$ and $\theta_{AC}$ components are analogous to the DC and AC components in electrical analysis. A DC amplification factor can then be defined as

$$P_{DC} = Bi\eta + 1 = \frac{\theta_{DC}(\eta)}{\theta_{DC}(0)} \geqslant 1 \quad \text{for} \quad \eta \geqslant 0. \tag{35}$$

Similarly an AC amplification factor can be defined as

$$P_{AC,n} = \cosh n\pi\eta + \frac{Bi}{n\pi}\sinh n\pi\eta$$

$$= \frac{\theta_{AC,n}(\xi, \eta)}{\theta_{AC,n}(\xi, 0)} \geqslant 1 \quad \text{for} \quad \eta \geqslant 0. \tag{36}$$

If the nonhomogeneous condition used to evaluate the Fourier coefficients is taken from the boundary at $\eta = \delta$, then $\theta$ can be expanded at $\delta$ as

$$\theta(\xi, \delta) = A_0(Bi\delta + 1) + \sum_{n=1}^{\infty} A_n \frac{n\pi}{Bi}\left(\cosh n\pi\delta + \frac{Bi}{n\pi}\sinh n\pi\delta\right)\cos n\pi\xi. \tag{37}$$

Here $A_0$ and $A_n$ can be found by using the orthogonality property of the eigenfunction, $\cos n\pi\xi$; for example,

$$A_0 = \int_0^1 \frac{\theta_{DC}(\delta)}{Bi\delta + 1}\,d\xi. \tag{38}$$

If the nonhomogeneous condition is taken at $\eta = 0$, the following equation will be used instead to find the Fourier coefficients:

$$\theta(\xi, 0) = a_0 + \sum_{n=1}^{\infty} a_n \frac{n\pi}{Bi}\cos n\pi\xi \tag{39}$$

where a new set of coefficients $a_0$ and $a_n$ have been designated in order to differentiate them from the $A_0$ and $A_n$ used earlier. Again, the orthogonality property of the eigenfunction, $\cos n\pi\xi$, enables $a_0$ to be expressed as

$$a_0 = \int_0^1 \theta_{DC}(0)\,d\xi. \tag{40}$$

Using equation (35), it can be shown that $A_0 = a_0$. Following a similar procedure, $A_n = a_n$. The analysis given here thus demonstrates that the Fourier coefficients are unique, independent of the location of the nonhomogeneous condition used to resolve them. It is also noted that the uniqueness of the solution for the present inverse problem has also been provided in the Cauchy–Kowalewsky theorem for Cauchy problems with analytic boundary conditions [25].

*Stability*

The Laplace equation (2) solved in this paper governs an equilibrium problem that does not have the stability problem that handicaps the solution of hyperbolic and parabolic equations [26]. The major concern in the present inverse problem is the iterative convergence of the Newton–Raphson procedures used in the solution of equations (15), (22), and (28). As has been shown, the Dirichlet problem requires solving equation (15) at each discrete point $\xi_i$. For this problem, if the initial guess $\eta_i^{(0)}$ is not accurate enough for equation (16) to converge, one can always continue the bisection algorithm to provide a more refined starting estimate $\eta_i^{(0)}$. However, in the solution of the Neumann (or Robin) condition problem, a marching scheme, based on the backward differenced forms of equations (22) and (28), has been proposed to evaluate a trial vector for $\eta_i^{(0)}$ in equation (16); see step (2), Example section. This trial vector must provide a sufficiently accurate starting value in order for the Newton–Raphson method to converge. Now, if $J^{-1}(\eta^{(i)})$ exists, then quadratic convergence is expected [27]. If the marching scheme yields a trial vector that is still inaccurate, then a convergent iteration might still be obtained by reducing the step size, $\Delta\xi$. However, another concern immediately arises with regard to the consistency in the numerical solution, as will now be discussed.

*Consistency*

Consider the Neumann-condition problem for example. If $\eta$ is continuously differentiable in equation (21), then

$$\frac{\eta_{i+1} - \eta_{i-1}}{2\Delta\xi} = \eta_i' + \varepsilon \tag{41}$$

where $\varepsilon$ designates the truncation error

$$\varepsilon = \eta_i''' \frac{\Delta\xi^2}{6} + 0(\Delta\xi^4). \tag{42}$$

Substituting equation (41) into (21) and using the fact that

$$\frac{\varepsilon(\varepsilon + 2\eta_i')}{1 + \eta_i'^2} < 1$$

the resulting equation can be expressed as

$$\text{LHS of equation (20)} + \frac{\varepsilon(\varepsilon + 2\eta_i')}{2(1 + \eta_i'^2)^{1/2}} + \text{higher-order terms} - \sum_{n=1}^{\infty} A_n n\pi\left(\frac{n\pi}{Bi}\cosh n\pi\eta_i + \sinh n\pi\eta_i\right) \times (\sin n\pi\xi_i)\eta_i''' \frac{\Delta\xi^2}{2}\left(\eta_i''' \frac{\Delta\xi^2}{2} + 2\eta_i'\right) = 0. \tag{43}$$

It is now seen that the finite-difference equation (21) is consistent as long as $\Delta\xi^2$ goes to zero faster than $\eta_i'''$ goes to infinity. Physically, that $\eta_i'''$ goes to infinity corresponds to a situation that the unknown boundary has high-frequency undulations. It can also be shown that the derived finite-difference form of the nonlinear ordinary differential equation (28) for the Robin subproblem is also consistent.

## NUMERICAL EXPERIMENT

For a test of the solution methods developed in this paper, a numerical experiment is performed that consists of three steps as follows:

(1) A boundary profile $f(\xi)$, see Fig. 4(a), is arbitrarily chosen for $S_4$ in the tests of all subproblems. This profile consists of three distinct features that enable a test of the strengths and limitations of the solution methods developed. The profile is made up of a shallow part at the left and a deep part at the right; the depth ratio being 1 : 3.5. There is also a rapid change of curvature of the slab profile near the deep end. With the boundary profile chosen, the temperature in the slab may be solved as a regular, boundary-value problem in the irregular region in order to find the temperature expression on surface $S_3$ [28].

(2) The temperature expression obtained in step (1) above is used to compute an array of temperatures, $\theta_N(\xi)$, which are then taken to be the exact (error-free) temperatures at $S_3$. Two arrays of inexact data are also generated for the purpose of simulating measurement errors. In this effort, because the surface temperatures measured by infra-red scanning in actual practice must be curve fitted before they can be used for locating the unknown boundary, a bias error is the worst one way encounter. A bias error of $\pm 5\%$ is thus introduced in the exact data to simulate measurement errors.

(3) From this point on, without using any knowledge of the $S_4$ profile, the surface temperature arrays obtained in step (2) above are used to determine the Fourier coefficients in the temperature expressions, and these expressions are, in turn, used to locate the boundaries using the methods given in this paper. Finally, those computed boundary positions are compared with the true boundary profile, $f(\xi)$, for error.

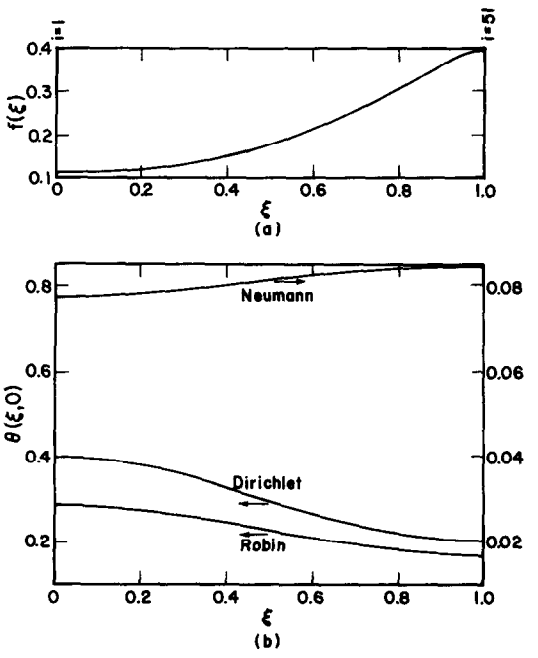


FIG. 4. Tested boundary configuration at $S_4$ and the resulting exact temperatures at $S_3$.

For all the tests made in this work, the range $0 \leqslant \xi \leqslant 1$ is discretized into $M$ equally spaced points. The step size, $\Delta\xi$, being related to $M$, is also tested for its effect on the convergence in the iterative solution. The number of terms taken in the Fourier series is determined by taking successively more terms in the partial sums of the Fourier series until convergence of the series is reached. It is also anticipated that an infra-red scanner will be used in practice to measure temperature, so the temperature resolution that will be considered later in testing the Neumann problem will be assessed on the basis of the precision that can be provided with that instrument [29].

## RESULTS AND DISCUSSION

The temperature curves plotted in Fig. 4(b) represent the exact data calculated at the surface $S_3$ as a result of the conditions imposed at the irregular boundary $S_4$, and these curves exhibit two different trends. For a Dirichlet or a Robin condition imposed at $S_4$, the hot spot on the surface appears where the slab is thin, which is not unexpected; however, for a Neumann condition at the boundary, this trend is reversed. These trends have also been found and explained in previous studies [17, 18].

The exact data given in Fig. 4(b) are then used to locate the unknown boundary $S_4$ for all three subproblems. Test results indicate that the unknown boundary can be located accurately for all three problems with the solution methods given in this paper. Also no difficulty was encountered in achieving convergent iteration by the Newton–Raphson method. For example, for a Robin condition at the unknown boundary, taking $M = 11$ (large step size) requires three iterations to get the boundary profile that is accurate to three significant figures. An increase of $M$ to 26 yields accuracy to four significant figures; the level of accuracy is improved to six significant figures for $M = 51$. The accuracies quoted here relate to the largest errors found over the boundary $S_4$, and the least accurate results are found near $\xi = 0.9$, a deep region of rapid change of boundary curvature as is not unexpected. The test of exact data is now complete.

The biased data are tested next, and it is found that the temperature difference between the two ends of the Neumann curve shown in Fig. 4(b) is about 17–28 times smaller than those for the Robin and Dirichlet curves. In fact, this temperature difference is close to the order of the bias error in the infra-red signal; the signal-to-noise ratio for the Neumann problem is so small that an accurate location of the boundary with the biased data is practically impossible in this case. For this reason, this Neumann problem will not be tested with the biased data; in the paragraphs that follow, the Dirichlet and Robin problems will be studied in detail because

they are the ones for which the inverse-problem solutions are useful.

As shown in Fig. 5, a bias error of + 5% in the surface temperature in the Dirichlet problem results in an underestimation of the depth of the unknown boundary, and this effect is particularly pronounced at the deep end of the boundary. For example, the error at $\xi = 1$ is 10.7%, while that at $\xi = 0$ is only 7.8%. Conversely, a bias error of −5% in the surface temperature results in an overestimation of the slab thickness; however, this time the error at $\xi = 0.96$ is an alarming 18% while that at $\xi = 0$ is still moderate (8.9%). Because of the deep boundary position for $S_4$ at $\xi = 1$, it is impossible to find the roots of equation (15) for points between $\xi = 0.98$ and 1. Mathematically, this can be explained by referring to the residual curves plotted in Fig. 6. The residual [that is, the LHS of equation (15)] for the noisy data is greater than zero for $\xi = 1$ for all $\eta$, a root thus fails to appear in this case. Also notice that this time the inverse solution is unable to reveal the rapid change of the curvature of the boundary near the deep end; see the curve for −4% in Fig. 5. It can thus be concluded that the solution presented in this paper works well for a shallow (unknown) boundary, whereas a deep boundary cannot be located accurately with this method. This limitation is explained below.

It has been mentioned earlier that the inverse problem solved in this paper can be considered a Cauchy-condition problem. For the present study, the

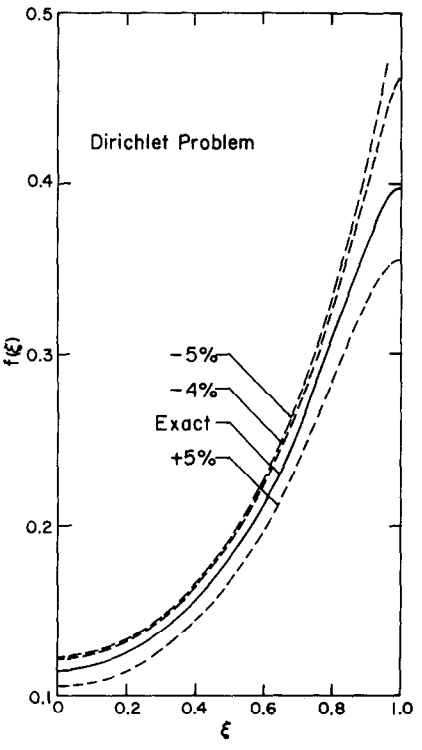


FIG. 5. A plot of the located boundary positions for the Dirichlet problem.

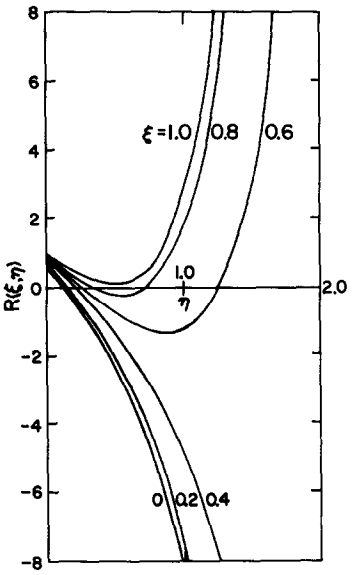


FIG. 6. A plot of residuals for the Dirichlet problem using noisy temperature data for input.

Cauchy conditions are used to derive the temperature expression, which is, in turn, used to locate the unknown boundary. Then, an error in the Cauchy data is expected to yield an inaccurate temperature expression, and as a result, the unknown boundary cannot be located accurately. The problem is further complicated by the fact that such a temperature error in the Cauchy data is not damped moving from the surface to the interior of the body. Then, the large error associated with deep boundaries should be considered as the nature of the problem [30, 31].

The same trends are found for a Robin condition imposed at the unknown boundary, see Fig. 7; however, the errors are larger than the Dirichlet problem. For example, the errors at $\xi = 0$ for the underestimated and overestimated positions are 10.8 and 11.8%, respectively, which correspond again to ±5% errors in the surface temperature. Furthermore, for a −5% error in the surface temperature, a refined boundary position using central difference can not be evaluated beyond $\xi = 0.78$ although a solution by backward difference can be carried out all the way up to $\xi = 0.98$, at which point the error of the overestimated depth is 29.9%. Both EAM and EFM methods mentioned earlier yield identical results, although the EFM methods is preferred in the solution of complicated geometries.

## CLOSING REMARKS

In closing, it should be noted that, in the plane slab example given above, the boundary conditions at the $\xi = 0$ and 1 planes have been chosen to be adiabatic because the surface temperature gradients at these points are zero. It is expected that, if the unknown boundary is located deep beneath the surface, then a

Table 1. A summary of equations for solving inverse problems in cylindrical coordinates

Temperature:

$$\theta(\rho,\phi)=D_0\left(\ln\rho-\frac{1}{Bi}\right)+\sum_{n=1}^{\infty}\left(\frac{n-Bi}{n+Bi}\rho^n+\rho^{-n}\right)(E_n\cos n\phi+F_n\sin n\phi)$$

where

$$\rho=\frac{r}{R_0},\quad Bi=\frac{hR_0}{k}$$

[see equations (10), (11) and (12) for definitions of $\theta$]

$\rho_i$s are roots of

(i) $$1-D_0\left(\ln\rho_i-\frac{1}{Bi}\right)-\sum_{n=1}^{\infty}\left(\frac{n-Bi}{n+Bi}\rho_i^n+\rho_i^{-n}\right)(E_n\cos n\phi_i+F_n\sin n\phi_i)=0$$

for a Dirichlet condition imposed at the unknown boundary,

(ii) $$\left[1+\left(\frac{\rho_{i+1}-\rho_{i-1}}{2\rho_i\Delta\phi}\right)^2\right]^{1/2}+\frac{D_0}{\rho_i}+\sum_{n=1}^{\infty}n\left\{\left[\frac{n-Bi}{n+Bi}\rho_i^{n-1}-\rho_i^{-(n+1)}\right](E_n\cos n\phi_i+F_n\sin n\phi_i)\right.$$
$$\left.+\left(\frac{\rho_{i+1}-\rho_{i-1}}{2\rho_i\Delta\phi}\right)\left[\frac{n-Bi}{n+Bi}\rho_i^{n-1}+\rho_i^{-(n+1)}\right](E_n\sin n\phi_i-F_n\cos n\phi_i)\right\}=0$$

for a Neumann condition imposed at the unknown boundary,

(iii) $$\left[1+\left(\frac{\rho_{i+1}-\rho_{i-1}}{2\rho_i\Delta\phi}\right)^2\right]^{1/2}Bi\left[1-D_0\left(\ln\rho_i-\frac{1}{Bi}\right)\right]+\frac{D_0}{\rho_i}+\sum_{n=1}^{\infty}n\left[\left\{\left(\frac{n-Bi}{n+Bi}\rho_i^{n-1}-\rho_i^{-(n+1)}\right)\right.\right.$$
$$\left.-\left[1+\left(\frac{\rho_{i+1}-\rho_{i-1}}{2\rho_i\Delta\phi}\right)^2\right]^{1/2}\frac{Bi}{n}\left(\frac{n-Bi}{n+Bi}\rho_i^n+\rho_i^{-n}\right)\right\}(E_n\cos n\phi_i+F_n\sin n\phi_i)$$
$$\left.+\left(\frac{\rho_{i+1}-\rho_{i-1}}{2\rho_i\Delta\phi}\right)\left[\frac{n-Bi}{n+Bi}\rho_i^{n-1}+\rho_i^{-(n+1)}\right](E_n\sin n\phi_i-F_n\cos n\phi_i)\right]=0$$

for a Robin condition imposed at the unknown boundary.

Table 2. A summary of equations for solving inverse problems in spherical coordinates

Temperature:

$$\theta(\rho,\phi)=\sum_{n=0}^{\infty}G_n\left[\frac{n+1-Bi}{n+Bi}\rho^n+\rho^{-(n+1)}\right]P_n(\cos\phi)$$

where

$$\rho=\frac{r}{R_0},\quad Bi=\frac{hR_0}{k},\quad P_n=\text{Legendre polynomial}$$

[see equations (10), (11) and (12) for definitions of $\theta$]

$\rho_i$s are roots of

(i) $$1-\sum_{n=0}^{\infty}G_n\left[\frac{n+1-Bi}{n+Bi}\rho_i^n+\rho_i^{-(n+1)}\right]P_n(\cos\phi_i)=0$$

for a Dirichlet condition imposed at the unknown boundary,

(ii) $$\left[1+\left(\frac{\rho_{i+1}-\rho_{i-1}}{2\rho_i\Delta\phi}\right)^2\right]^{1/2}+\sum_{n=0}^{\infty}G_n\left\{\left[\frac{n+1-Bi}{n+Bi}n\rho_i^{n-1}-(n+1)\rho_i^{-(n+2)}\right]P_n(\cos\phi_i)\right.$$
$$\left.+\left(\frac{\rho_{i+1}-\rho_{i-1}}{2\rho_i\Delta\phi}\right)\left[\frac{n+1-Bi}{n+Bi}\rho_i^{n-1}+\rho_i^{-(n+2)}\right]\sin\phi_iP_n'(\cos\phi_i)\right\}=0$$

for a Neumann condition imposed at the unknown boundary,

(iii) $$\left[1+\left(\frac{\rho_{i+1}-\rho_{i-1}}{2\rho_i\Delta\phi}\right)^2\right]^{1/2}Bi+\sum_{n=0}^{\infty}G_n\left[\left\{\left[\frac{n+1-Bi}{n+Bi}n\rho_i^{n-1}-(n+1)\rho_i^{-(n+2)}\right]\right.\right.$$
$$\left.-\left[1+\left(\frac{\rho_{i+1}-\rho_{i-1}}{2\rho_i\Delta\phi}\right)^2\right]^{1/2}Bi\left[\frac{n+1-Bi}{n+Bi}\rho_i^n+\rho_i^{-(n+1)}\right]\right\}P_n(\cos\phi_i)$$
$$\left.+\left(\frac{\rho_{i+1}-\rho_{i-1}}{2\rho_i\Delta\phi}\right)\left[\frac{n+1-Bi}{n+Bi}\rho_i^{n-1}+\rho_i^{-(n+2)}\right]\sin\phi_iP_n'(\cos\phi_i)\right]=0$$

for a Robin condition imposed at the unknown boundary.

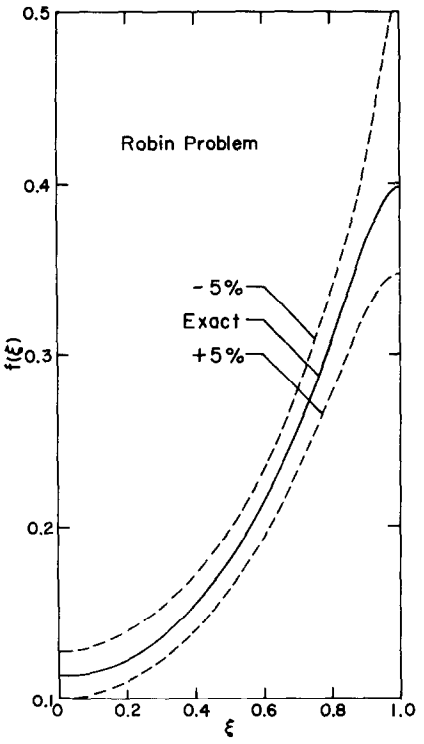


FIG. 7. A plot of the located boundary positions for the Robin problem.

zero temperature gradient at the surface may not be served as clues for those planes being adiabatic. In such an event, these boundaries at $\xi = 0$ and 1 must be moved to the physical boundaries of the slab and proper conditions imposed there for modelling.

It may also be mentioned that, although the plane slab has been chosen as an example for tests, the methods developed for solution in this paper are general and applicable to other geometries. A summary of equations useful for the solution of other problems in cylindrical and spherical coordinates is provided in Tables 1 and 2. In order to test the usefulness of the presently developed solution methods in nondestructive testing of flaws and cavities by infra-red scanning, a physical experiment has also been carried out. The solution methods work successfully as reported in [32].

*Acknowledgments*—The research reported here was performed under the auspices of the U.S. National Science Foundation grant MEA-8309514. Mr S. L. Yang assisted in obtaining numerical solutions for a portion of examples. Professor M. C. K. Yang provided support in statistical analysis.

## REFERENCES

1. G. Stolz, Jr, Numerical solutions to an inverse problem of heat conduction for simple shapes, *J. Heat Transfer* **82,** 20–26 (1960).
2. I. Frank, An application of least squares method to the solution of the inverse problem of heat conduction, *J. Heat Transfer* **85,** 378–379 (1963).
3. E. M. Sparrow, A. Haji-Sheikh and T. S. Lundgren, The inverse problem in transient heat conduction, *J. appl. Mech.* **86,** 369–375 (1964).
4. O. R. Burggraf, An exact solution of the inverse problem in heat conduction theory and applications, *J. Heat Transfer* **86,** 373–382 (1964).
5. J. R. Cannon, Determination of certain parameters in heat conduction problems, *J. Math. Anal. Appl.* **8,** 188–201 (1964).
6. J. V. Beck, The inverse problem in transient heat conduction, *J. appl. Mech.* **87,** 472–473 (1965).
7. L. I. Deverall and R. S. Channapragada, A new integral equation for heat flux in inverse heat conduction, *J. Heat Transfer* **88,** 327–328 (1966).
8. J. V. Beck, Surface heat flux determination using an integral method, *Nucl. Engng Des.* **7,** 170–178 (1968).
9. J. V. Beck, Nonlinear estimation applied to the nonlinear inverse heat conduction problem, *Int. J. Heat Mass Transfer* **13,** 703–716 (1970).
10. M. C. K. Yang and C. K. Hsieh, A three component method of data analysis for nondestructive testing by infrared scanning, *Proc. Soc. photo-opt. Instrum. Engrs* **95,** 212–216 (1976).
11. C. K. Hsieh, M. C. K. Yang, E. A. Farber and A. Jorolan, A feasibility study to test structure integrity by infrared scanning technique. In *Thermal Conductivity*, Vol. 14, p. 521. Plenum Press, New York (1976).
12. M. M. Chen, C. O. Pedersen and J. C. Chato, On the feasibility of obtaining three-dimensional information from thermographic measurements, *J. biomech. Engng* **99,** 58–64 (1978).
13. N. N. Malakhov, Identification methods of boundary conditions found from the solution of the inverse heat-conduction problem, *Inzh.-Fiz. Zh.* **33,** 1062–1066 (1977).
14. N. I. Nikitenko and Y. M. Kolodnyi, Numerical solution of the inverse heat-conduction problem for determining thermal constants, *Inzh.-Fiz. Zh.* **33,** 1058–1061 (1977).
15. C. K. Hsieh and W. A. Ellingson, The feasibility of using infrared scanning to test flaws in ceramic materials. In *Thermal Conductivity*, Vol. 15, p. 11. Plenum Press, New York (1978).
16. J. V. Beck, Criteria for comparison of methods of solution of the inverse heat conduction problem, *Nucl. Engng Des.* **53,** 11–22 (1979).
17. C. K. Hsieh and K. C. Su, A methodology of predicting cavity geometry based on the scanned surface temperature data-prescribed surface temperature at the cavity side, *J. Heat Transfer* **102,** 324–329 (1980).
18. C. K. Hsieh and K. C. Su, A methodology of predicting cavity geometry based on the scanned surface temperature data-prescribed heat flux at the cavity side, *J. Heat Transfer* **103,** 42–46 (1981).
19. K. C. Woo and L. C. Chow, Inverse heat conduction by direct inverse Laplace transform. *Numer. Heat Transfer* **4,** 499–504 (1981).
20. C. K. Hsieh, X. A. Wang and S. L. Yang, Infrared scanning thermography for a quantitative detection of cavities in a plane slab and a rectangular prism, *J. nondestruct. Evaluation* **3,** 64–74 (1982).
21. V. P. Mishin and O. M. Alifanov, Inverse problems of heat exchange-fields of application in the planning and testing of technical objects, *Inzh.-Fiz. Zh.* **42,** 181–192 (1982).
22. V. I. Iordanov and A. P. Steward, A method and a computer program for determining the thermal diffusivity in a solid slab, *Appl. Math. Model.* **8,** 169–178 (1984).
23. P. M. Morse and H. Feshbach, *Methods of Theoretical Physics*, Part I, Chap. 6. McGraw-Hill, New York (1953).
24. E. Kreyszig, *Advanced Engineering Mathematics*, 5th edn, Chap. 9. John Wiley, New York (1983).
25. I. G. Petrovsky, *Lectures on Partial Differential Equations*, Chap. 1. Interscience, New York (1954).
26. D. A. Anderson, J. C. Tannehill and R. H. Pletcher, *Computational Fluid Mechanics and Heat Transfer*, Chap. 3. McGraw-Hill, New York (1984).

27. R. L. Burden, D. J. Faires and A. C. Reynolds, *Numerical Analysis*, p. 448. Prindle, Weber & Schmidt, Boston (1981).
28. B. A. Finlayson, *The Method of Weighted Residuals and Variational Principles*, Chap. 2. Academic Press, New York (1972).
29. E. T. Wong and C. K. Hsieh, Use of infrared scanners to make accurate temperature and position measurements, ASME Paper 83-HT-85 (1983).
30. J. Hammard, *Lectures on Cauchy's Problem in Linear Partial Differential Equations*, Book I, Chap. II. Dover, New York (1952).
31. A. Carasso and A. P. Stone, *Improperly Posed Boundary Value Problems*. Pitman, London (1975).
32. C. K. Hsieh, Z. Z. Lin and S. L. Yang, An inverse problem technique for detecting irregular cavities in circular cylinders by infrared scanning, *J. nondestruct. Evaluation* **4**, 131–138 (1985).

## UNE METHODE GENERALE POUR LA SOLUTION DES PROBLEMES INVERSES DE CONDUCTION THERMIQUE AVEC DES GEOMETRIES DE SYSTEMES PARTIELLEMENT INCONNUES

**Résumé**—On introduit un problème auxiliaire dans la solution des problèmes inverses de conduction thermique avec des géométries pas complètement spécifiées. En résolvant la position de la frontière inconnue soumise à une condition de Dirichlet, on est conduit à la résolution d'une équation algébrique non-linéaire. L'imposition des conditions de Neumann ou de Robin à la frontière inconnue nécessite la résolution d'une équation différentielle du premier ordre et non linéaire. La méthode fournit des résultats précis pour des données exactes, tandis que des erreurs de mesure rendent le problème de Neumann insoluble. Les problèmes de Dirichlet et de Robin sont résolvables, et pour ces problèmes, les erreurs dans la recherche de la frontière augmentent avec sa profondeur, et l'on recherche la nature de ce problème.

## EINE ALLGEMEINE METHODE ZUR LÖSUNG INVERSER WÄRMELEITPROBLEME MIT TEILWEISE UNBEKANNTEN SYSTEMGEOMETRIEN

**Zusammenfassung**—Bei der Lösung inverser Wärmeleitprobleme mit nicht vollständig definierter Geometrie werden Hilfsprobleme eingeführt. Nochmaliges Bestimmen des Ortes der unbekannten Begrenzung—Gegenstand einer Dirichlet-Bedingung—führt zu der Lösung einer nichtlinearen algebraischen Gleichung. Die Neumann- oder Robin-Bedingung, angewandt an der unbekannten Begrenzung, erfordert das Lösen einer gewöhnlichen, nichtlinearen Differentialgleichung 1. Ordnung. Diese Methode führt zu genauen Ergebnissen für exakte Daten, während Meßfehler das Neumann'ssche Problem unlösbar machen. Die Dirichlet- und Robin-Probleme sind noch lösbar. Ihre Natur wird untersucht, wobei die Fehler in den untersuchten Grenzen mit der Tiefe zunehmen.

## ОБЩИЙ МЕТОД РЕШЕНИЯ ОБРАТНЫХ ЗАДАЧ ТЕПЛОПРОВОДНОСТИ В СИСТЕМАХ С ЧАСТИЧНО ИЗВЕСТНОЙ ГЕОМЕТРИЕЙ

**Аннотация**—Для решения обратных задач теплопроводности в системе с не совсем точно известной геометрией предложено использование вспомогательной задачи. При заданном условии Дирихле для положения неизвестной границы необходимо решить нелинейное алгебраическое уравнение. Наложение на неизвестную границу условия Неймана или Робина требует решения нелинейных обыкновенных дифференциальных уравнений первого порядка. Метод дает хорошие результаты при наличии точных данных, в то время как из-за ошибок измерений задача Неймана становится неразрешимой. Задачи же Дирихле и Робина разрешимы, но в этом случае ошибки возрастают с увеличением размеров тела.